ACS APPLIED MATERIALS & INTERFACES

Letter

www.acsami.org

Pt Electrodes Enable the Formation of μ_4-O Centers in MOF-5 from Multiple Oxygen Sources

Minyuan M. Li and Mircea Dincă*

Department of Chemistry, Massachusetts Institute of Technology, Cambridge, Massachusetts 02139, United States

Supporting Information

ABSTRACT: The μ_4-O^{2-} ions in the $Zn_4O(O_2C{-})_6$ secondary building units of Zn_4O(1,4-benzenedicarboxylate)$_3$ (MOF-5) electrodeposited under cathodic bias can be sourced from nitrate, water, and molecular oxygen when using platinum gauze as working electrodes. The use of $Zn(ClO_4)_2{\cdot}6H_2O$, anhydrous $Zn(NO_3)_2$, or anhydrous $Zn(CF_3SO_3)_2$ as Zn^{2+} sources under rigorous control of other sources of oxygen, including water and O_2, confirm that the source of the μ_4-O^{2-} ions can be promiscuous. Although this finding reveals a relatively complicated manifold of electrochemical processes responsible for the crystallization of MOF-5 under cathodic bias, it further highlights the importance of hydroxide intermediates in the formation of the $Zn_4O(O_2C{-}R)$ secondary building units in this iconic material and is illustrative of the complicated crystallization mechanisms of metal−organic frameworks in general.

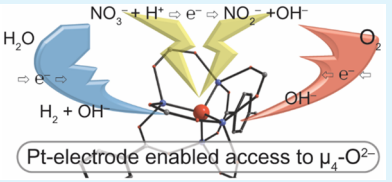

KEYWORDS: *metal−organic frameworks, electrochemistry, electrodeposition, mechanism of reactions, crystals*

Electrode surfaces critically influence the observed potential of kinetically sluggish redox couples, such as the pH-changing reactions that are commonly used for electrochemically induced crystallizations: water or oxoanion reduction.[1] In addition to their electrochemical (i.e., kinetic) influence on the electrodeposition process, electrode surfaces also play key roles in the nucleation and growth of the electrodeposited materials. With this unique offering of controllable variables, electrodeposition becomes an attractive synthetic and mechanistic tool for studying the formation of various crystalline solids.[2,3] We have been interested in using electrodeposition to control and study the formation of metal−organic frameworks (MOFs),[4−7] whose synthesis is still largely empirical and relies on mechanisms of nucleation and growth that are still poorly understood.[8−10]

We showed previously that electrochemical reduction of probases such as nitrate (eq 1) on fluorine-doped tin oxide (FTO) leads to the deposition of a thin film of $Zn_4O(BDC)_3$ (MOF-5; BDC = 1,4-benzenedicarboxylate; Figure 1).[11] Other phases in the Zn-BDC system are also accessible by varying the applied potential, which ultimately affects the identity and activity of various solution species.[12] Platinum electrodes are particularly effective for dialing either proton or nitrate reduction events. This allows the modulation of probase at a given potential with concurrent selective crystallization of pure phases and the formation of layered MOF heterostructures by simply dialing the applied potential.[13] This unprecedented phase differentiation is important toward utilization of MOFs as functional materials and toward understanding fundamental aspects of solid-phase transformations involved in MOF crystallization. As the use of electrochemical techniques for MOF synthesis receives increasing attention,[14−18] mechanistic investigations become critical in guiding future studies. In this work, we further examine the reactivity native to platinum

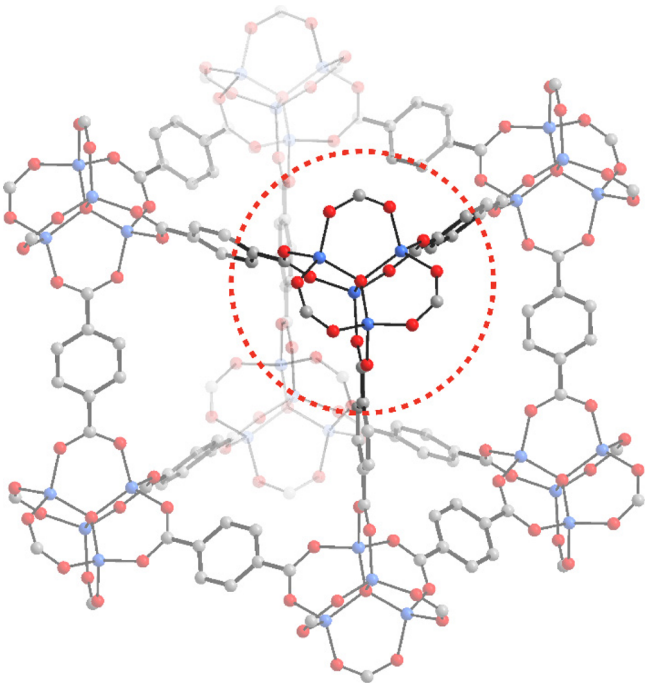

Figure 1. Portion of the crystal structure of MOF-5, highlighting a $Zn_4O(O_2C{-})_6$ cluster. Blue, red, and gray sphere represent Zn, O, and C atoms, respectively. Hydrogen atoms are omitted for clarity.

Special Issue: Hupp 60th Birthday Forum

Received: December 30, 2016
Accepted: February 8, 2017
Published: February 8, 2017

DOI: 10.1021/acsami.6b16821
ACS Appl. Mater. Interfaces XXXX, XXX, XXX−XXX

electrodes and show that the source of the μ_4-O^{2-} ions in MOF-5 is more promiscuous than previously anticipated.

$$NO_3^- + H_2O + 2e^- \rightarrow NO_2^- + 2OH^- \quad (1)$$

Despite its iconic status in the field, or perhaps because of it, MOF-5 continues to challenge the fundamental understanding of MOFs. It was recently shown, for instance, that Zn^{2+} ions dynamically bind solvent molecules and display fast exchange between 4-, 5- and 6-coordination in the as-synthesized material.[19] One of the outstanding enigmas related to MOF-5's secondary building unit (SBU) is the provenance of the μ_4-O^{2-} that bridges the four zinc ions in $Zn_4O(O_2C-)_6$. Some reports have speculated on the origin of these key bridging ions, surmising that they are products of acid−base reactions involving water,[20] by analogy with studies on the formation of molecular basic zinc carboxylate species, $Zn_4O(O_2C-R)$ (R = alkyl).[21,22] A subsequent mechanistic study effected under anhydrous conditions suggested that NO_3^- ions were instead the source of μ_4-O^{2-} under solvothermal growth.[23] Other reports also showed peroxides facilitating the assembly of $Zn_4O(O_2C-)_6$ clusters in the presence of triethylamine at room temperature.[24,25]

$$NO_3^- + H_2BDC + 2e^- \rightarrow NO_2^- + H_2O + BDC^{2-} \quad (2)$$

We showed previously that NO_3^- can function as probase (eq 2) and the sole source of μ_4-O^{2-} in anhydrous *N*,*N*-dimethylformamide (DMF) when using either FTO or Pt as the working electrode (Figure 2 and Figure S1).[11,12] This led to

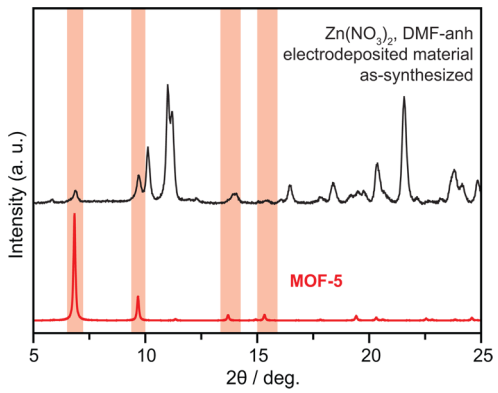

Figure 2. PXRD pattern of a sample deposited at −1.50 V on a Pt gauze electrode in DMF-anh with 0.1 M tetra-*n*-butylammonium hexafluorophosphate ($TBAPF_6$) for 90 min (reagent concentrations: $[Zn(NO_3)_2]$ = 150 mM, $[H_2BDC]$ = 50 mM). The PXRD pattern of MOF-5 is simulated.[24] Sample PXRD pattern after isolation in air can be found in Figure S1.

an intriguing question: would MOF-5 form at all in the absence of nitrate? The relevance of this question stems from the fact that MOF-5 crystallization in the presence of nitrate is preceded by the formation of metastable layered zinc hydroxide phases such as $Zn_5(OH)_8(H_2O)_2\cdot(NO_3)_2$. Because the nitrate anions in these intermediate phases are weakly bound and susceptible to topotactic exchange,[12,26] we reasoned that MOF-5 may indeed be accessible in the absence of nitrate, from a combination of acid−base reactivity between H_2BDC and zinc hydroxides (eq 3), and electrochemical generation of HO^- by water reduction, for instance (eq 4).

$$3H_2BDC + [Zn_4(OH)_8] \rightarrow 7H_2O + \text{MOF-5} \quad (3)$$

$$H_2O + e^- \rightarrow \frac{1}{2}H_2 + OH^- \quad (4)$$

We performed a series of experiments aimed at eliminating NO_3^- from the deposition medium. First, we tested a deposition bath containing no nitrate, with $Zn(ClO_4)_2\cdot 6H_2O$ as the source of Zn^{2+}. Applying a potential of −1.50 V (all electrochemical potentials in this work are referenced to the $Ag/Ag(cryptand)^+$ couple, see the Supporting Information) to a Pt gauze electrode in solutions of H_2BDC, tetra-*n*-butylammonium hexafluorophosphate ($TBAPF_6$), and $Zn(ClO_4)_2\cdot 6H_2O$ produced crystalline deposits with weak but well-resolved PXRD peaks corresponding to MOF-5 after 150 min of continuous electrolysis (Figure 3 and Figure S3). In

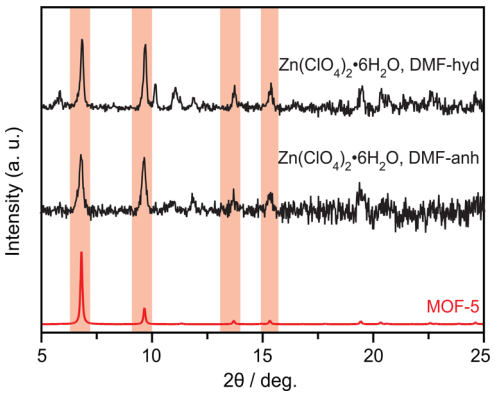

Figure 3. Normalized PXRD patterns of samples deposited at −1.50 V on Pt gauze electrodes in DMF-anh and in DMF-hyd for 150 min (reagent concentrations: $[Zn(ClO_4)_2\cdot 6H_2O]$ = 150 mM, $[H_2BDC]$ = 50 mM). DMF-hyd is a solution of DMF-anh with 1% v/v of water.

other words, under conditions where water is the sole source of oxygen atoms, MOF-5 still forms, albeit in lower quantity (Figures S7 and S9). Although perchlorate anions can, in principle, function as probases in a similar manner to nitrate, cyclic voltammetry experiments of tetrabutylammonium perchlorate (TBAP), and H_2BDC solutions (i.e., solutions identical to the deposition bath safe for the presence of Zn^{2+}) confirmed that perchlorate is not reduced under these conditions on Pt cathodes (Figures S5 and S6).[27] Because we have observed the formation of MOF-5 under cathodic electrolysis in the absence of nitrate, H_2O (and HO^-) must be able to act as the sole source for μ_4-O^{2-}.

Seeing that H_2O is itself a competent probase, we turned our attention to molecular oxygen, O_2, as a potential probase. Under our experimental conditions, we found the O_2 reduction potential at approximately −0.70 V (Figure 4), much more anodically shifted than the reduction of Zn^{2+} to Zn metal. Cyclic voltammetry of an O_2-saturated DMF-anh solution indicated one-electron reduction to the superoxide anion radical.[28] The large peak-to-peak separation between this event and the oxidation event observed on the reverse potential scan is likely due to adsorption of superoxide onto the Pt electrode surface (eq 5; $E_{p,c}$ = −1.19 V, $E_{p,a}$ = −0.42 V).[29,30] In the presence of H_2BDC, a new cathodic process is observed at −0.97 V. This likely corresponds to H_2 evolution from protons originating either from the carboxylic acid or from O_2-derived hydrogen peroxide (eqs 6 and 7).[31] Notably, the formation of hydroxide from superoxide or peroxide should be thermodynamically favorable under our deposition potential (eqs 8 and 9).[32]

DOI: 10.1021/acsami.6b16821
ACS Appl. Mater. Interfaces XXXX, XXX, XXX−XXX

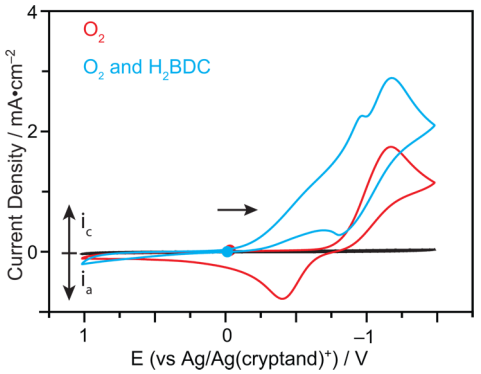

Figure 4. Cyclic voltammograms at 100 mV/s in DMF-anh (solvent background, black) of a saturated O_2 solution (red) and a solution of 15 mM H_2BDC with saturated O_2 (blue) on a Pt electrode. The $O_2/O_2^{(-\cdot)}$ couple (eq 4) is observed at $E_{p,c} = -1.19$ V, $E_{p,a} = -0.42$ V).[29,33] After the addition of H_2BDC, the major reduction peak remained at −1.19 V. A weak and broad cathodic feature at approximately $E_{p,c} = -0.60$ V was observed with decreasing peak current in each subsequent scans. The peak at $E_{p,c} = -0.97$ V likely corresponds to H_2 evolution.

Under these conditions, the O_2 reduction peak remains unshifted with $E_{p,c} = -1.19$ V. The disappearance of the anodic peak at −0.42 V suggests that the relative concentration of stable reduced product is low in the now protic environment, possibly due to a fast chemical step, such as the rapid disproportionation of superoxide to peroxide and O_2 (eq 7).

$$O_2 + e^- \leftrightarrow O_2^{(-\cdot)} \quad (5)$$

$$O_2^{(-\cdot)} + H^+ \rightarrow HO_2 \quad (6)$$

$$2HO_2 \rightarrow O_2 + H_2O_2 \quad (7)$$

$$HO_2 + H^+ + 3e^- \rightarrow 2OH^- \quad (8)$$

$$H_2O_2 + 2e^- \rightarrow 2OH^- \quad (9)$$

Saturating a $Zn(ClO_4)_2{\cdot}6H_2O$/DMF-anh deposition bath with O_2 before bulk electrolysis at −1.50 V led to the formation of MOF-5 in 30 min, whereas the control experiment under N_2 gas showed only zinc deposition (Figures 5 and Figure S7) with. Moreover, MOF-5 formation under O_2 is independent of the Zn^{2+} source: replacing $Zn(ClO_4)_2{\cdot}6H_2O$ with anhydrous $Zn(CF_3SO_3)_2$, which contain electrochemically inactive triflate anions,[27] also led to competent formation of MOF-5 upon electrolysis at −1.50 V (Figure 6 and Figure S11). Because O_2 is the only reactive oxygen species at this potential, it must serve as the sole source of μ_4-O^{2-} ions for the formation of MOF-5. It should be noted, however, that the mechanism for the formation of the Zn_4O cluster in the presence of O_2 may yet be different than when the μ_4-O^{2-} ions come from nitrate or water. Indeed, O_2 reduction in the presence of metal cations is known to create peroxide species such as $Zn(O_2)$, which may undergo chemical transformations leading to alternative crystallization pathways compared to using either nitrate or water as the probase.[29,30]

CONCLUSIONS

Using tunable variables in the process of cathodic electrodeposition, we were able to show that μ_4-O^{2-} in the $Zn_4O(O_2C-)_6$ SBUs of MOF-5 can be accessed not just from nitrate, but also water and oxygen. On platinum, the well-documented redox behaviors of both proton and oxygen reduction reactions were necessary to analyze the electrochemical behavior in the deposition solution. The relative crystallinity of the MOF obtained from reactions rigorously utilizing water or oxygen as the probase is lower than the crystallinity observed for material deposited from nitrate. This emphasizes the potential importance of previously identified layered zinc hydroxy-nitrates as intermediates during MOF-5 deposition under cathodic bias. Establishing the role of various probases, including O_2 as demonstrated here, will prove important in future exploits of cathodic electrodeposition, where varying other experimental parameters such as temperature and pressure may reveal additional aspects of nucleation and crystal growth in the canonic Zn-BDC system.

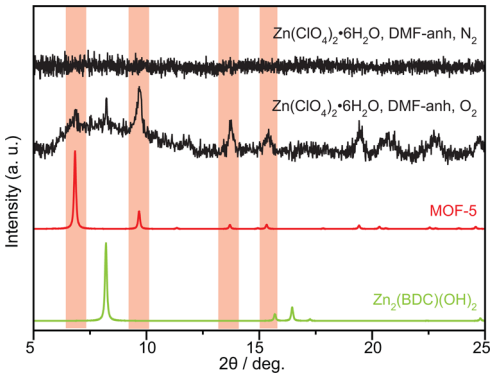

Figure 5. PXRD patterns of samples deposited in DMF-anh on Pt gauze electrodes at −1.50 V for 30 min (reagent concentrations $[Zn(ClO_4)_2{\cdot}6H_2O]$ = 75 mM, $[H_2BDC]$ = 25 mM). The working compartment was sparged with the indicated gas for 30 min before electrolysis and kept at a pressure slightly above 1 atm. throughout the deposition process. The PXRD pattern of $Zn_2(BDC)(OH)_2$ was simulated with a preferential orientation along (001).[34] The PXRD pattern of MOF-5 was simulated without additional parameters.[24] See also Figure S7.

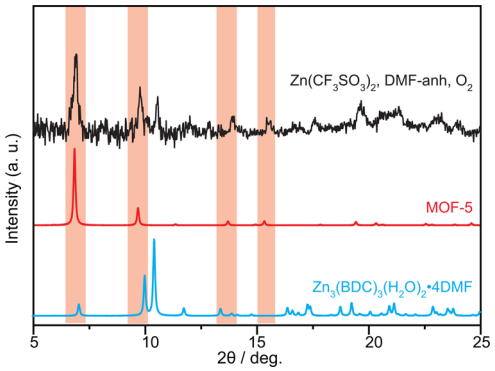

Figure 6. PXRD patterns of a sample deposited in DMF-anh on Pt gauze electrodes at −1.50 V for 30 min (reagent concentrations: $[Zn(CF_3SO_3)_2]$ = 75 mM, $[H_2BDC]$ = 25 mM). The working compartment was assembled in a N_2 glovebox, sealed with parafilm, transferred outside, sparged with O_2 for 30 min before electrolysis, and kept under a pressure slightly above 1 atm. throughout the deposition process. PXRD patterns of MOF-5 and $Zn_3(BDC)_3(H_2O)_2{\cdot}4DMF$ are simulated.[24,35] See also Figure S11.

ASSOCIATED CONTENT

Supporting Information

The Supporting Information is available free of charge on the ACS Publications website at DOI: 10.1021/acsami.6b16821.

DOI: 10.1021/acsami.6b16821
ACS Appl. Mater. Interfaces XXXX, XXX, XXX−XXX

Chronoamperograms indicating deposition current traces, cyclic voltammograms of control experiments showing the stability of anions under electrolytic conditions, PXRD patterns of films obtained under different deposition times, hydration levels, applied potentials, and substrate concentrations (PDF)

AUTHOR INFORMATION

Corresponding Author

*E-mail: mdinca@mit.edu.

ORCID

Minyuan M. Li: 0000-0002-4078-9435

Mircea Dincă: 0000-0002-1262-1264

Present Address

[a]Department of Chemistry, Massachusetts Institute of Technology, 77 Massachusetts Avenue, Cambridge, MA 02139, USA.

Funding

All experimental work was supported by the U.S. Department of Energy, Office of Science, Office of Basic Energy Sciences (U.S. DOE-BES, Award DE-SC0006937). M.D. thanks 3 M, the Sloan Foundation, and the Research Corporation for Science Advancement (Cottrell Scholar Program) for Non-Tenured Faculty Funds and the MISTI-Belgium Fund for travel support. Grants from the NSF (CHE-9808061, DBI-9729592) provided instrument support to the DCIF at MIT. M.L. was partially supported by an NSF Graduate Research Fellowship Program under Grant 1122374. We thank K. Armburst for assistance with coulometry.

Notes

The authors declare no competing financial interest.

REFERENCES

(1) Xu, S.; Melendres, C. A.; Kamrath, M. A. Structure and Morphology of Electrodeposited $CaCO_3$: X-Ray Diffraction and Microscopy Studies. *J. Electrochem. Soc.* **1999**, *146* (9), 3315.

(2) Kang, D.; Kim, T. W.; Kubota, S. R.; Cardiel, A. C.; Cha, H. G.; Choi, K.-S. Electrochemical Synthesis of Photoelectrodes and Catalysts for Use in Solar Water Splitting. *Chem. Rev.* **2015**, *115* (23), 12839−12887.

(3) Govindaraju, G. V.; Wheeler, G. P.; Lee, D.; Choi, K.-S. Methods for Electrochemical Synthesis and Photoelectrochemical Characterization for Photoelectrodes. *Chem. Mater.* **2017**, *29* (1), 355−370.

(4) Al-Kutubi, H.; Gascon, J.; Sudhölter, E. J. R.; Rassaei, L. Electrosynthesis of Metal-Organic Frameworks: Challenges and Opportunities. *ChemElectroChem* **2015**, *2*, 462.

(5) Li, W.-J.; Tu, M.; Cao, R.; Fischer, R. A. Metal−organic Framework Thin Films: Electrochemical Fabrication Techniques and Corresponding Applications & Perspectives. *J. Mater. Chem. A* **2016**, *4* (32), 12356−12369.

(6) Bradshaw, D.; Garai, A.; Huo, J. Metal-Organic Framework Growth at Functional Interfaces: Thin Films and Composites for Diverse Applications. *Chem. Soc. Rev.* **2012**, *41* (6), 2344−2381.

(7) Shekhah, O.; Liu, J.; Fischer, R. A.; Wöll, C. MOF Thin Films: Existing and Future Applications. *Chem. Soc. Rev.* **2011**, *40* (2), 1081−1106.

(8) Biswal, D.; Kusalik, P. G. Probing Molecular Mechanisms of Self-Assembly in Metal−Organic Frameworks. *ACS Nano* **2017**, *11* (1), 258−268.

(9) Patterson, J. P.; Abellan, P.; Denny, M. S.; Park, C.; Browning, N. D.; Cohen, S. M.; Evans, J. E.; Gianneschi, N. C. Observing the Growth of Metal−Organic Frameworks by in Situ Liquid Cell Transmission Electron Microscopy. *J. Am. Chem. Soc.* **2015**, *137* (23), 7322−7328.

(10) Greer, H. F.; Liu, Y.; Greenaway, A.; Wright, P. A.; Zhou, W. Synthesis and Formation Mechanism of Textured MOF-5. *Cryst. Growth Des.* **2016**, *16* (4), 2104−2111.

(11) Li, M.; Dincă, M. Reductive Electrosynthesis of Crystalline Metal-Organic Frameworks. *J. Am. Chem. Soc.* **2011**, *133* (33), 12926−12929.

(12) Li, M.; Dincă, M. On the Mechanism of MOF-5 Formation under Cathodic Bias. *Chem. Mater.* **2015**, *27* (9), 3203−3206.

(13) Li, M.; Dincă, M. Selective Formation of Biphasic Thin Films of Metal−organic Frameworks by Potential-Controlled Cathodic Electrodeposition. *Chem. Sci.* **2014**, *5* (1), 107−111.

(14) Hod, I.; Bury, W.; Karlin, D. M.; Deria, P.; Kung, C.-W.; Katz, M. J.; So, M.; Klahr, B.; Jin, D.; Chung, Y.-W.; Odom, T. W.; Farha, O. K.; Hupp, J. T. Directed Growth of Electroactive Metal-Organic Framework Thin Films Using Electrophoretic Deposition. *Adv. Mater.* **2014**, *26* (36), 6295−6300.

(15) Stassen, I.; Styles, M.; Van Assche, T.; Campagnol, N.; Fransaer, J.; Denayer, J.; Tan, J.-C.; Falcaro, P.; De Vos, D.; Ameloot, R. Electrochemical Film Deposition of the Zirconium Metal−Organic Framework UiO-66 and Application in a Miniaturized Sorbent Trap. *Chem. Mater.* **2015**, *27* (5), 1801−1807.

(16) Worrall, S. D.; Mann, H.; Rogers, A.; Bissett, M. A.; Attfield, M. P.; Dryfe, R. A. W. Electrochemical Deposition of Zeolitic Imidazolate Framework Electrode Coatings for Supercapacitor Electrodes. *Electrochim. Acta* **2016**, *197*, 228−240.

(17) Li, W.-J.; Liu, J.; Sun, Z.-H.; Liu, T.-F.; Lü, J.; Gao, S.-Y.; He, C.; Cao, R.; Luo, J.-H. Integration of Metal-Organic Frameworks into an Electrochemical Dielectric Thin Film for Electronic Applications. *Nat. Commun.* **2016**, *7*, 11830.

(18) Li, M. M. *Cathodic Electrodeposition of Metal−Organic Frameworks*; Massachusetts Institute of Technology: Cambridge, MA, 2015.

(19) Brozek, C. K.; Michaelis, V. K.; Ong, T.-C.; Bellarosa, L.; López, N.; Griffin, R. G.; Dincă, M. Dynamic DMF Binding in MOF-5 Enables the Formation of Metastable Cobalt-Substituted MOF-5 Analogues. *ACS Cent. Sci.* **2015**, *1* (5), 252−260.

(20) Tranchemontagne, D.; Hunt, J.; Yaghi, O. Room Temperature Synthesis of Metal-Organic Frameworks: MOF-5, MOF-74, MOF-177, MOF-199, and IRMOF-0. *Tetrahedron* **2008**, *64* (36), 8553−8557.

(21) Gordon, R. M.; Silver, H. B. Preparation and Properties of Tetrazinc μ_4-Oxohexa-μ-Carboxylates (Basic Zinc Carboxylates). *Can. J. Chem.* **1983**, *61* (6), 1218−1221.

(22) Clegg, W.; Harbron, D. R.; Homan, C. D.; Hunt, P. A.; Little, I. R.; Straughan, B. P. Crystal Structures of Three Basic Zinc Carboxylates Together with Infrared and FAB Mass Spectrometry Studies in Solution. *Inorg. Chim. Acta* **1991**, *186* (1), 51−60.

(23) Hausdorf, S.; Wagler, J.; Mossig, R.; Mertens, F. O. R. L. Proton and Water Activity-Controlled Structure Formation in Zinc Carboxylate-Based Metal Organic Frameworks. *J. Phys. Chem. A* **2008**, *112* (33), 7567−7576.

(24) Li, H.; Eddaoudi, M.; O'Keeffe, M.; Yaghi, O. M. Design and Synthesis of an Exceptionally Stable and Highly Porous Metal-Organic Framework. *Nature* **1999**, *402*, 276−279.

(25) Zhao, H.; Song, H.; Chou, L. Facile Synthesis of MOF-5 Structure with Large Surface Area in the Presence of Benzoyl Peroxide by Room Temperature Synthesis. *Mater. Chem. Phys.* **2014**, *143* (3), 1005−1011.

(26) Zheng, C. M.; Greer, H. F.; Chiang, C. Y.; Zhou, W. Z. Microstructural Study of the Formation Mechanism of Metal-Organic Framework MOF-5. *CrystEngComm* **2014**, *16* (6), 1064−1070.

(27) House, H. O.; Feng, E.; Peet, N. P. Comparison of Various Tetraalkylammonium Salts as Supporting Electrolytes in Organic Electrochemical Reactions. *J. Org. Chem.* **1971**, *36* (16), 2371−2375.

(28) The saturation concentration of dissolved oxygen in DMF under 1 atm of O_2 is at 4.8 mM, a much lower concentration than the one of probase in solution. See refs 29 and 30.

(29) Sawyer, D. T.; Chiericato, G.; Angelis, C. T.; Nanni, E. J.; Tsuchiya, T. Effects of Media and Electrode Materials on the

DOI: 10.1021/acsami.6b16821
ACS Appl. Mater. Interfaces XXXX, XXX, XXX−XXX

Electrochemical Reduction of Dioxygen. *Anal. Chem.* **1982**, *54* (11), 1720−1724.
(30) Sawyer, D. T. *Oxygen Chemistry*; Oxford University Press: New York, 1991.
(31) Morrison, M. M.; Roberts, J. L.; Sawyer, D. T. Oxidation-Reduction Chemistry of Hydrogen Peroxide in Aprotic and Aqueous Solutions. *Inorg. Chem.* **1979**, *18* (7), 1971−1973.
(32) Pegis, M. L.; Roberts, J. A. S.; Wasylenko, D. J.; Mader, E. A.; Appel, A. M.; Mayer, J. M. Standard Reduction Potentials for Oxygen and Carbon Dioxide Couples in Acetonitrile and N,N-Dimethylformamide. *Inorg. Chem.* **2015**, *54* (24), 11883−11888.
(33) Feroci, G.; Roffia, S. On the Reduction of Oxygen in Dimethylformamide. *J. Electroanal. Chem. Interfacial Electrochem.* **1976**, *71* (2), 191−198.
(34) Carton, A.; Mesbah, A.; Aranda, L.; Rabu, P.; François, M. New Metastable Hybrid Phase, $Zn_2(OH)_2(C_8H_4O_4)$, Exhibiting Unique Oxo-Penta-Coordinated Zn(II) Atoms. *Solid State Sci.* **2009**, *11* (4), 818−823.
(35) Edgar, M.; Mitchell, R.; Slawin, a M.; Lightfoot, P.; Wright, P. A. Solid-State Transformations of Zinc 1,4-Benzenedicarboxylates Mediated by Hydrogen-Bond-Forming Molecules. *Chem. - Eur. J.* **2001**, *7* (23), 5168−5175.

DOI: 10.1021/acsami.6b16821
ACS Appl. Mater. Interfaces XXXX, XXX, XXX−XXX